Modeling of fixed wing UAV and design of multivariable flight controller using PID tuned by local optimal control

To cite this article: Eslam Nabil Mobarez *et al* 2019 *IOP Conf. Ser.: Mater. Sci. Eng.* **610** 012016

Modeling of fixed wing UAV and design of multivariable flight controller using PID tuned by local optimal control

Eslam Nabil Mobarez [1, 3], Amr Sarhan [2], and Mahmoud Mohamed Ashry [1]

[1]Department of Optoelectronics and Control, Military Technical College, Cairo, Egypt
[2]Aircraft electrical equipment, Military Technical College, Cairo, Egypt

[3] E-mail. eslammob85@hotmail.com

Abstract. Ultrastick-25e is an unmanned air vehicle fabricated by University of Minnesota. The traditional PI control was purposed for Ultrastick-25e in both longitudinal and lateral branches. Throughout this paper, PI and PID controllers are purposed for Ultrastick-25e in both longitudinal and lateral branches of linear and nonlinear model. Two tuning methods are utilized to enhance the autopilot response of Ultrastic-25e UAV. The autopilot system robustness is tested by measuring the capability of the controllers in rejecting the wind disturbances, and attenuating the noises generated from the sensors. The genetic algorithm optimizer is utilized as the first method for tuning the PI and PID controllers and enhance the performance and robustness of the system. The Local Optimal Control (LOC) is utilized as the second method for tuning the PI and PID after that. The essential contribution of this paper is utilizing local optimal control for tuning parameters of PI and PID on UAVs for the first time. The comparative study of the results assure the superiority of this tuning method over the other tuning methods used.

Keywords: Equations of motion, Mathematical modeling, linearization, Genetic algorithm, Local optimal control, PID tuning techniques.

1. Introduction

The neoteric researches in advanced guidance, control, and navigation have been grown in the last decade [1 - 4]. The utilization of autonomous Unmanned Aerial Vehicles (UAV) opens the gate to a vast diversity of both military and civil applications [5, 6]. The researchers' goals are flight robustness and acceptable performance for their control system design of the UAVs [4, 5]. Several control methods are utilized to control Ultrasticke-25e based on mathematical modeling [7, 8]. PI conventional controller is designed in 2015 to enhance the performance of the PI controller designed by university of Minnesota [9].

Two PI/PID tuning methods are proposed in this paper to enhance the control response. The genetically tuned PI and PID controllers are utilized as the first tuning method. The local optimal control (LOC) is utilized as the second tuning method for PI and PID controllers' parameters for the underlying flight control system. Tuning of PID controller parameters based on LOC for gas turbine engine (GTE) has already been discussed in [8]. The results obtained at that time showed robustness to model uncertainties and an acceptable output response even in the presence of disturbance and noise [10, 11]. Based on these previous results, this tuning technique is used in this paper for the first time to design the flight controller of fixed wing UAV. In this paper, the autopilot controlled using PID tuned by

LOC realizes an acceptable and an agreeable output response even in the presence of disturbance and noise.

This paper is outlined as following:

The mathematical model for Ultrasticke-25e is introduced in section two. The third section presents linearization at certain flight condition. The design of the flight control systems are applied in section four. Section five shows the simulation results and the comparative analysis of longitudinal and lateral channels for the linear model considering the effect of disturbance and noise. The simulation results and the comparative analysis of longitudinal and lateral channels considering the effect of disturbance and noise are configured for the nonlinear model in section sex. The last section is for conclusions.

2. Ultrastick-25e mathematical model derivation

The equations of motion include the differential equations describing the aircraft dynamics [6, 7]. The equations of motion can be divided into two categories which are kinematic and dynamic equations. Kinematic equations describe the angular orientation and velocities of the body axes system with respect to the gravity vector. Dynamic equations consist of summation of forces and moments act on the aircraft starting from newton's law of motion. The equations of motions are derived by taking into account the physical laws of motion. The transpose of the state vector X can be defined as follows:

$$X^T = [V_T\ \beta\ \ \alpha\ \phi\ \theta\ \psi\ p\ q\ r\ lat\ long\ h]$$

where: $\boldsymbol{V_T}$ is the aircraft velocity vector, β is the side slip angle, $\boldsymbol{\alpha}$ is the angle of attack, $\boldsymbol{\phi}$ is the Roll angle, $\boldsymbol{\theta}$ is the pitch angle, $\boldsymbol{\psi}$ is the heading angle, h is the altitude, p is the roll rate, q is the pitch rate, r is the yaw rate, $\boldsymbol{lat}$ latitude, $\boldsymbol{long}$ longitude.

Force equation is the starting point for the derivation of the equations representing the aircraft motion will be the vector form of newton's second law of motion as follows:

$$F = \frac{d(mV_T)}{dt} \tag{1}$$

where: F is the sum of external forces acting on the aircraft, m is the mass of the aircraft which assumed to be constant.

The derivative of an arbitrary vector V_T referred to the body frame which is rotating in relative to inertial frame with angular velocity ω can be obtained using the theorem of Coriolis as follows:

$$F = m\,(\frac{dV_T}{dt} + \omega \otimes V_T) \tag{2}$$

The different flight vectors can be expressed along the body-coordinate axes as follows:

$$V_T = U\,\hat{\imath} + V\,\hat{\imath} + W\,\hat{k} \tag{3}$$

where (U, V, W) are velocity component

$$\omega = p\,\hat{\imath} + q\,\hat{\imath} + r\,\hat{k} \tag{4}$$

where (p, q, r) are angular velocity component

$$\omega \otimes V_T = \begin{bmatrix} \hat{\imath} & \hat{\imath} & k \\ p & q & r \\ U & V & W \end{bmatrix} = \hat{\imath}\,(q\,W - r\,V) - \hat{\imath}(pW - Ur) + \hat{k}(p\,V - q\,U) \tag{5}$$

Substituting from equation (3), (4), (5) into equation (2) deducing the force and the components of the aircraft translational motion as follow in equations (6), and (7-9) respectively.

$$F = m\big(\dot{U}\,\hat{\imath} + \dot{V}\,\hat{\imath} + \dot{W}\,\hat{k} + \hat{\imath}\,(q\,W - r\,V) - \hat{\imath}(pW - Ur) + \hat{k}(p\,V - q\,U)\big) \tag{6}$$

$$F_X = m\,(\dot{U} + q\,W - V\,r) \tag{7}$$

$$F_y = m\,(\dot{V} + P\,W - U\,r) \tag{8}$$

$$F_Z = m\,(\,\dot{W} + p\,V - U\,q) \tag{9}$$

where, (F_X, F_y, F_z) are the force components.

Moment equation is used and the angular momentum and inertia matrix are defined as:

$$M = \frac{d(H)}{dt} \tag{10}$$

Where M is the summation of all moments, H is the angular momentum,

$$M = \frac{d(H)}{dt} + \omega \otimes H \tag{11}$$

$$H = I * \omega \tag{12}$$

Where I is the moment of inertia

$$I = \begin{bmatrix} I_{XX} & -I_{Xy} & -I_{XZ} \\ -I_{yX} & I_{YY} & -I_{yz} \\ -I_{ZX} & -I_{zy} & I_{ZZ} \end{bmatrix}, \omega = p\,\hat{\imath} + q\,\hat{\imath} + r\,\hat{k} \tag{13}$$

Substituting from equation (13) into equation (12)

$$H = \begin{bmatrix} I_{XX} & 0 & -I_{XZ} \\ 0 & I_{YY} & 0 \\ -I_{ZX} & 0 & I_{ZZ} \end{bmatrix} \begin{bmatrix} p \\ q \\ r \end{bmatrix} = \begin{bmatrix} I_{XX}p - I_{XZ}r \\ I_{XX}q \\ -I_{ZX}\,p + I_{ZZ}r \end{bmatrix} \tag{14}$$

So the derivative of angular momentum,

$$\frac{d(H)}{dt} = \begin{bmatrix} I_{XX}\dot{p} - I_{XZ}\dot{r} \\ I_{XX}\dot{q} \\ -I_{ZX}\,\dot{p} + I_{ZZ}\dot{r} \end{bmatrix} \tag{15}$$

Substituting from equation (14) and (15) into equation (11) deducing the moment component of the aircraft as in equations (16-18), where (M_X, M_y, M_z) are the moment components. As the aircraft is symmetric about XZ plane, then $(I_{Xy} = I_{yz} = 0)$.

$$M_X = I_{XX}\dot{p} - I_{Xz}(\dot{r} + p\,q) + \left(I_{zz} - I_{yy}\right) q\,r \tag{16}$$

$$M_y = I_{yy}\dot{q} - I_{Xz}(p^2 + r^2) + (I_{xx} - I_{zz})\,p\,r \tag{17}$$

$$M_z = I_{zz}\dot{r} - I_{Xz}\dot{p} + p\,q\left(I_{yy} - I_{xx}\right) + I_{Xz}q\,r \tag{18}$$

The equations of motion have been deduced for body fixed axes system for simplicity. Unfortunately, the positions and directions of the aircraft cannot be described relative to a moving body axes reference frame, so we refer this body axes system to a basic frame of reference whose origin is being fixed at the center of the earth called Earth axis system.

The angular orientation of the body axis with respect to the Earth axis depends upon the orientation sequence. This sequence of rotations is explained as follows:

- Rotate the Earth axesX_E,Y_E, Z_E through azimuthal angle ψ about the axis Z_E to reach some intermediate axes X_1,Y_1, Z_1.
- Rotate the axes X_1,Y_1, Z_1through elevation angle $\boldsymbol{\theta}$ about the axis Y_1 to reach some intermediate axes X_2,Y_2, Z_2.
- Rotate the axes X_2,Y_2, Z_2through bank angle $\boldsymbol{\phi}$ about the axis X_2 to reach the body axes X_B,Y_B, Z_B.

The corresponding transformation matrices using the direction cosines technique are obtained in reference to the following Fig. (1). as follows:

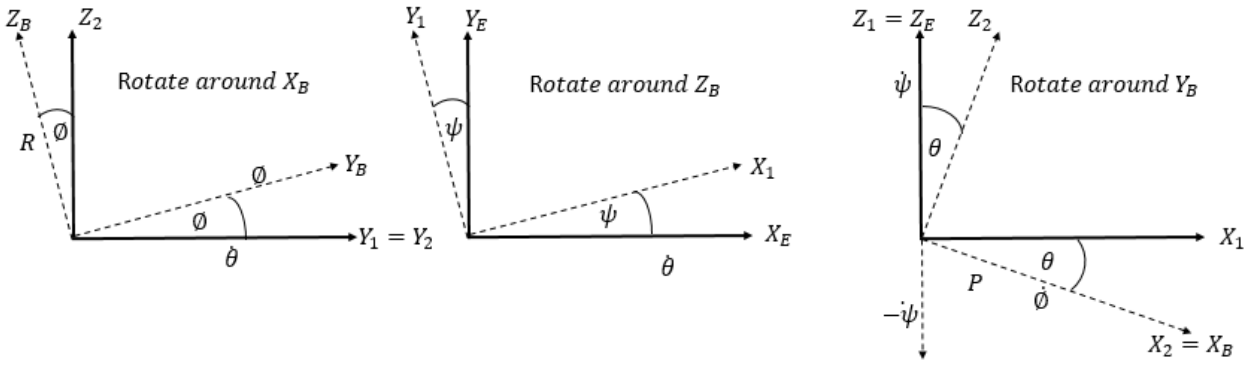

Figure 1. Relationships between body and inertial axes system

$$\begin{bmatrix} X \\ Y \\ Z \end{bmatrix}_{BODY} = \left[DCM_{\psi} DCM_{\theta} DCM_{\phi}\right] \begin{bmatrix} X \\ Y \\ Z \end{bmatrix}_{EARTH} \tag{19}$$

$$\begin{bmatrix} X_1 \\ Y_1 \\ Z_1 \end{bmatrix} = \begin{bmatrix} \cos\psi & \sin\psi & 0 \\ -\sin\psi & \cos\psi & 0 \\ 0 & 0 & 1 \end{bmatrix} \begin{bmatrix} X_E \\ Y_E \\ Z_E \end{bmatrix} \tag{20}$$

$$\begin{bmatrix} X_2 \\ Y_2 \\ Z_2 \end{bmatrix} = \begin{bmatrix} \cos\theta & 0 & -\sin\theta \\ 0 & 1 & 0 \\ \sin\theta & 0 & \cos\theta \end{bmatrix}, \begin{bmatrix} X_1 \\ Y_1 \\ Z_1 \end{bmatrix} \tag{21}$$

$$\begin{bmatrix} X_1 \\ Y_1 \\ Z_1 \end{bmatrix} = \begin{bmatrix} 1 & 0 & 0 \\ 0 & \cos\phi & \sin\phi \\ 0 & -\sin\phi & \cos\phi \end{bmatrix} \begin{bmatrix} X_2 \\ Y_2 \\ Z_2 \end{bmatrix} \tag{22}$$

$$DCM_{\psi} = \begin{bmatrix} \cos\psi & \sin\psi & 0 \\ -\sin\psi & \cos\psi & 0 \\ 0 & 0 & 1 \end{bmatrix}, DCM_{\theta} = \begin{bmatrix} \cos\theta & 0 & -\sin\theta \\ 0 & 1 & 0 \\ \sin\theta & 0 & \cos\theta \end{bmatrix}, DCM_{\phi} = \begin{bmatrix} 1 & 0 & 0 \\ 0 & \cos\phi & \sin\phi \\ 0 & -\sin\phi & \cos\phi \end{bmatrix} \tag{23}$$

The complete transformation matrix direction cosine matrix (DCM) is obtained as follows

$$DCM = DCM_{\psi}\, DCM_{\theta}\, DCM_{\phi}$$

$$= \begin{bmatrix} \cos\psi\cos\theta & \sin\psi\cos\theta & - \\ \cos\psi\sin\theta\sin\phi - \sin\psi\sin\phi & \sin\psi\sin\theta\sin\phi + \cos\psi\cos\phi & \cos \\ \cos\psi\sin\theta\cos\phi + \sin\psi\sin\phi & \sin\psi\sin\theta\sin\phi - \cos\psi\sin\phi & \cos \end{bmatrix} \tag{24}$$

$$\begin{bmatrix} X \\ Y \\ Z \end{bmatrix}_{BODY} = \left[DCM_{\psi} DCM_{\theta} DCM_{\phi}\right] \begin{bmatrix} X \\ Y \\ Z \end{bmatrix}_{EARTH} \tag{25}$$

The kinematic equations can be obtained as follow

$$p = \dot{\phi} - \dot{\psi}\sin\theta \tag{26}$$

$$q = \dot{\theta}\cos\phi + \dot{\psi}\cos\theta\sin\phi \tag{27}$$

$$r = -\dot{\theta}\sin\phi + \dot{\psi}\cos\theta\cos\phi \tag{28}$$

$$\dot{\phi} = p + \dot{\psi}\sin\theta \tag{29}$$

Multiply equation (27) by $(\boldsymbol{\sin\phi})$

$$q\sin\phi = \dot{\theta}\cos\phi\sin\phi + \dot{\psi}\cos\theta\sin^2\phi \tag{30}$$

and equation (28) by $(\boldsymbol{\cos\phi})$

$$r\cos\phi = -\dot{\theta}\sin\phi\cos\phi + \dot{\psi}\cos\theta\cos^2\phi \tag{31}$$

Sum the two previous equation to each other

$$q\sin\phi + r\cos\phi = \dot{\theta}\cos\phi\sin\phi + \dot{\psi}\cos\theta\sin^2\phi - \dot{\theta}\sin\phi\cos\phi + \dot{\psi}\cos\theta\cos^2\phi \tag{32}$$

$$\dot{\psi}\cos\theta = q\sin\phi + r\cos\phi \quad (33)$$

$$\dot{\psi} = q\sin\phi\sec\theta + r\cos\phi\sec\theta \quad (34)$$

Multiply equation (27) by $(\boldsymbol{\cos\phi})$

$$q\cos\phi = \dot{\theta}\cos^2\phi + \dot{\psi}\cos\theta\sin\phi\cos\phi \quad (35)$$

and equation (28) by $(-\boldsymbol{\sin\phi})$

$$r\cos\phi = -\dot{\theta}\sin^2\phi + \dot{\psi}\cos\theta\sin\phi\cos\phi \quad (36)$$

Sum the two previous equation to other

$$\dot{\theta} = q\cos\phi - r\sin\phi \quad (37)$$

In the Earth reference axis system, the position of the aircraft center of gravity (c.g.) is represented by the inertial position vector$P_0(t)$. The transformation matrix DCM that takes vectors from the Earth reference frame to the body frame is given by Eq. (24). Since the Earth reference frame and body frame are orthogonal and the transformation is a pure rotation, then the DCM matrix is an orthogonal matrix and consequently its transpose (DCM') is equal to its inverse. Therefore, the absolute velocity of aircraft c.g. in Earth reference frame is given by:

$$\dot{P}_0 = \text{DCM}' \begin{bmatrix} U \\ V \\ W \end{bmatrix} \qquad P_X = \dot{P}_n\,,\ P_Y = \dot{P}_e,\ P_Z = \dot{h}$$

$$\dot{P}_n = U\,cos\theta\,cos\psi + V(-cos\varphi\,sin\psi + sin\varphi\,sin\theta cos\psi) + W\,(sin\varphi\,sin\psi + cos\varphi\,sin\theta cos\psi) \quad (38)$$

$$\dot{P}_e = U\,cos\theta\,sin\,\psi + V(cos\varphi\,cos\psi + sin\varphi\,sin\theta sin\psi) + W\,(-sin\varphi\,cos\psi + cos\varphi\,sin\theta sin\psi) \quad (39)$$

$$\dot{h} = U\,sin\theta - V(cos\varphi\,sin\psi + sin\varphi cos\theta) + W\,(cos\,\varphi\,cos\theta) \quad (40)$$

where ($\dot{P}_n$,$\dot{P}$, $\dot{h}$) are the inertial position components.

The forces and moments acting on the aircraft are defined in terms of dimensionless aerodynamic coefficients and the flight dynamic pressure as follows:

For longitudinal force

$$X = \bar{q}\,S\,C_X \quad (41)$$

For lateral force

$$Y = \bar{q}\,S\,C_Y \quad (42)$$

For vertical force

$$Z = -\,\bar{q}\,S\,C_Z \quad (43)$$

For roll moment

$$L = \bar{q}\,S\,B\,C_L \quad (44)$$

For pitch moment

$$M = \bar{q}\,S\,\bar{c}\,C_M \quad (45)$$

For yaw moment

$$N = \bar{q}\,S\,B\,C_N \quad (46)$$

where $\bar{q} = \frac{\rho\,v^2}{2}$ is the dynamic pressure, S is the wing reference area, B is the wing span (length), $\bar{c}$ is the wing mean geometric chord, the various dimensionless coefficients CX, CY, CZ, CL, CM, CN are dependent on the aerodynamic angles, rates of change of these angles, the components p, q, r of the body angular velocity and on the control surface deflections. Although the effect of airspeed v is accounted for through the dynamic pressure $\bar{q}$, the aerodynamic coefficients are still airspeed dependent. Also, they are dependent on other factors, such as engine power level.

$$C_X = C_X(\propto) + C_{X_q}(\propto)\frac{c\,q}{2\,V} + C_{X\,\delta e}(\propto)\,\delta e \tag{47}$$

$$C_Y = C_{Y_0} + C_{Y\,\beta}(\beta) + C_{Y_p}(\beta)\frac{b\,p}{2\,V} + C_{Y_r}\frac{b\,r}{2\,V} + C_{Y\,\delta a}\delta a + C_{Y\,\delta r}\delta r \tag{48}$$

$$C_Z = C_z(\propto) + C_{z_q}(\propto)\frac{c\,q}{2\,V} + C_{z\,\delta e}(\propto)\,\delta e \tag{49}$$

$$C_L = C_L\ +\ C_{L_\beta}\,\beta + C_{L_p}\frac{b\,p}{2\,V} + C_{L_r}\frac{b\,r}{2\,V} + C_{L_{\delta a}}\delta a + C_{L_{\delta r}}\delta r \tag{50}$$

$$C_M = C_{m_0}\ +\ C_{m_\propto} + C_{m_q}\frac{c\,q}{2\,V} + C_{m\,\delta e}\,\delta e \tag{51}$$

$$C_N = C_N\ +\ C_{N_\beta}\,\beta + C_{N_p}\frac{b\,p}{2\,V} + C_{N_r}\frac{b\,r}{2\,V} + C_{N_{\delta a}}\delta a + C_{N_{\delta r}}\delta r \tag{52}$$

The gravitational forces following components:

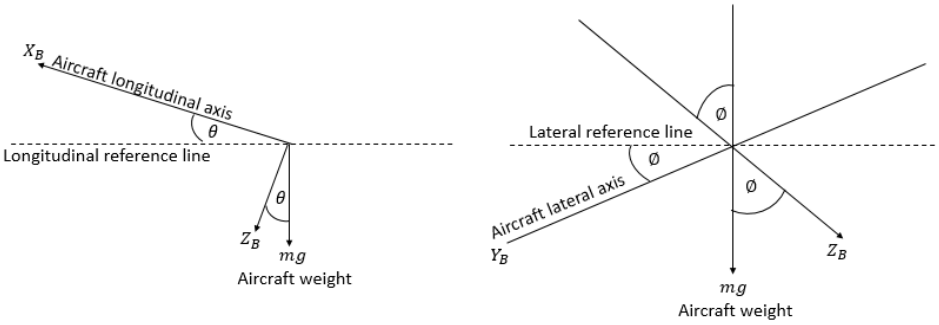

Figure 2. Gravity axes with respect to body axes

$$G_X = -mg\sin\theta \tag{53}$$

$$G_Y = mg\cos\theta\sin\phi \tag{54}$$

$$G_Z = mg\cos\theta\cos\phi \tag{55}$$

So the external forces acting on the aircraft can be re-represented as:

$$X = F_X + G_X$$

$$\bar{q}\,S\,C_X = m\left(\dot{U} + q\,W - V\,r\right) + -mg\sin\theta \tag{56}$$

$$Y = F_Y + G_Y$$

$$\bar{q}\,S\,C_Y = m\left(\dot{V} + P\,W - U\,r\right) + mg\cos\theta\sin\phi \tag{57}$$

$$Z = F_Z + G_Z$$

$$-\,\bar{q}\,S\,C_Z = m\,(\dot{W} + p\,V - U\,q)mg\cos\theta\cos\phi \tag{58}$$

So the external moment acting on the aircraft can be re-represented as:

$$L = M_X$$

$$\bar{q}\,S\,B\,C_L = I_{XX}\dot{p} - I_{Xz}(\dot{r} + p\,q) + \left(I_{zz} - I_{yy}\right)q\,r \tag{59}$$

$$M = M_Y$$

$$\bar{q}\,S\ \bar{c}\ C_M = I_{yy}\dot{q} - I_{Xz}(p^2 + r^2) + (I_{xx} - I_{zz})\,p\,r \tag{60}$$

$$N = M_Z$$

$$\bar{q}\,S\ B\,C_N = I_{zz}\dot{r} - I_{Xz}\dot{p} + p\,q\left(I_{yy} - I_{xx}\right) + I_{Xz}q\,r \tag{61}$$

3. Linearization of the nonlinear equations of motion

The mathematical modeling of longitudinal branch was proved analytically through nonlinear equations of motion for Ultrasticke-25e. This model is linearized at certain flight conditions and validated it to nonlinear model [7].

3.1. Lateral channel

In this section the analytical linearization of roll dynamics can be derived to find a plant to be controlled. From the deduced nonlinear equations of motion, the following equations can be obtained.

$$\dot{\phi} = p + \dot{\psi}\sin\theta \tag{62}$$

$$\dot{\psi} = q\sin\phi\sec\theta + r\cos\phi\sec\theta \tag{63}$$

So the

$$\dot{\phi} = p + q\sin\phi\tan\theta + r\cos\phi\tan\theta \tag{64}$$

From the equation (64) the equation of q represent as follows:

$$q = \frac{\dot{\phi} - p - r\cos\phi\tan\theta}{\sin\phi\tan\theta} \tag{65}$$

Taking the derivative of the equation (64) the following equation is obtained

$$\ddot{\phi} = \dot{p} + \dot{q}\sin\phi\tan\theta + q(\cos\phi\tan\theta + q\sin\phi\,sec^2\theta) + \dot{r}\cos\phi\tan\theta + r(\cos\phi\,sec^2\theta - \sin\phi\tan\theta) \tag{66}$$

Substituting from equation (65) in equation (66) the following equation is obtained

$$\ddot{\phi} = \dot{p} + \dot{q}\sin\phi\tan\theta + \frac{\dot{\phi}-p-r\cos\phi\tan\theta}{\sin\phi\tan\theta}(\cos\phi\tan\theta + q\sin\phi\,sec^2\theta) + \dot{r}\cos\phi\tan\theta + r(\cos\phi\,sec^2\theta - \sin\phi\tan\theta) \tag{67}$$

And from equation (59, 60, 61) the following equations are deduced:

$$\dot{q} = \Gamma_5\,p\,r - \Gamma_6\,(p^2 - r^2) + \frac{\rho v^2 s\,c}{2\,I_y}(C_{m_0} + C_{m_\propto} + C_{m_q}\frac{c\,q}{2\,V} + C_{m_{\delta e}}\,\delta e) \tag{68}$$

$$\dot{p} = \Gamma_1\,p\,q - \Gamma_2\,q\,r + \frac{\rho v^2 s\,b}{2}(C_{Y_0} + C_{Y_\beta}(\beta) + C_{Y_p}(\beta)\frac{b\,p}{2\,V} + C_{Y_r}\frac{b\,r}{2\,V} + C_{Y_{\delta a}}\delta a + C_{Y_{\delta r}}\delta r) \tag{69}$$

To get the transfer function of $\frac{\phi}{\delta a}$, so neglect the deflection of rudder and elevator in equation (68) and (69)

$$\dot{r} = \Gamma_7\,p\,q - \Gamma_1\,q\,r + \frac{\rho v^2 s\,b}{2}(C_{Y_0} + C_{Y_\beta}(\beta) + C_{Y_p}(\beta)\frac{b\,p}{2\,V} + C_{Y_r}\frac{b\,r}{2\,V} + C_{Y_{\delta a}}\delta a + C_{Y_{\delta r}}\delta r) \tag{70}$$

where:

$\Gamma_1 = (I_y - I_z)I_z - I_{xz}^2$, $\Gamma_2 = (I_x - I_y + I_z) - I_{xz}$

$\Gamma_5 = \frac{(I_z - I_x)}{I_y}$, $\Gamma_6 = \frac{(I_{xz})}{I_y}$, $\Gamma_7 = \frac{1}{I_y}$

and:

S = 0.3097m^2, c = 0.25, b =1.27 m, ρ = 1.19 at 100 ft. p = 4.25*10^{-25}, r =-4.173 *10^{-24}, ϕ =-0.0017, v = 17, θ= 0.0538, q =6.076*10^{-23}, β = -1.3714*10^{-22}, I_{xx}=0.0715, I_{yy}=0.0864, I_{zz}=0.1536, I_{xz} = 0.0140, C_{m_0}=-0.0278, $C_{m_\propto}$=-0.7230, C_{m_q}=-13.5664, $C_{m_{\delta e}}$=-0.8488, C_{Y_0} = 0.1, C_{Y_β}=-0.0545, $C_{Y_p}(\beta)$=-0.4496, C_{Y_r}=0.1086, $C_{Y_{\delta a}}$=-0.1646,

From the derivation of the linearization the obtained transfer function of roll angle is given in equation (71)

$$G_1(z) = \frac{\varphi}{\delta a} = \frac{-0.04612\,z}{z^2 - 1.737\,z + 0.7366} \tag{71}$$

And transfer function of roll rate is given in equation (72)

$$G_2(z) = \frac{P}{\delta a} = \frac{-2.297}{z - 0.7389} \tag{72}$$

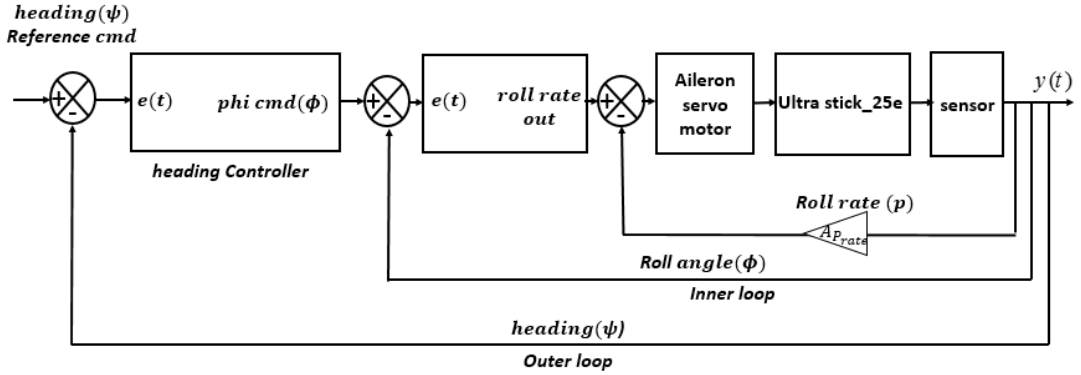

Figure 3. Lateral Autopilot

3.2. Longitudinal channel

In this section the analytical linearization of pitch dynamics can be derived to find a plant to be controlled. From deduced nonlinear equations of motion, the following equations can be obtained.

$$\dot{\theta} = q\cos\phi - r\sin\phi \tag{73}$$

$$\ddot{\theta} = \dot{q}\cos\phi - q\sin\phi - r\cos\phi - \dot{r}\sin\phi \tag{74}$$

$$q = \frac{\dot{\theta} + r\sin\phi}{\cos\phi} \tag{75}$$

$$q = \frac{\dot{\theta}}{\cos\phi} + +r\tan\phi \tag{76}$$

$$\ddot{\theta} = \dot{q}\cos\phi - \sin\phi\left(\frac{\dot{\theta}}{\cos\phi} + +r\tan\phi\right) - r\cos\phi - \dot{r}\sin\phi \tag{77}$$

$$\ddot{\theta} = \dot{q}\cos\phi - \tan\phi\,\dot{\theta} + +r\tan\phi\sin\phi - r\cos\phi - \dot{r}\sin\phi \tag{78}$$

And from equation (59, 60, 61), the following equations are deduced:

$$\dot{q} = \Gamma_5 p r - \Gamma_6(p^2 - r^2) + \frac{\rho v^2 s c}{2 I_y}\left(C_{m_0} + C_{m_\alpha} + C_{m_q}\frac{c q}{2V} + C_{m_{\delta e}}\delta e\right) \tag{79}$$

$$\dot{r} = \Gamma_7 p q - \Gamma_1 q r + \frac{\rho v^2 s b}{2}\left(C_{Y_0} + C_{Y_\beta}(\beta) + C_{Y_p}(\beta)\frac{b p}{2V} + C_{Y_r}\frac{b r}{2V} + C_{Y_{\delta a}}\delta a + C_{Y_{\delta r}}\delta r\right) \tag{80}$$

$$\begin{aligned}\ddot{\theta} = {} & \left[\Gamma_5 p r - \Gamma_6(p^2 - r^2) + \frac{\rho v^2 s c}{2 I_y}\left(C_{m_0} + C_{m_\alpha} + C_{m_q}\frac{c q}{2V} + C_{m_{\delta e}}\delta e\right)\right]\cos\phi - \tan\phi\,\dot{\theta} \\ & + +r\tan\phi\sin\phi - r\cos\phi \\ & - \left[\Gamma_7 p q - \Gamma_1 q r + \frac{\rho v^2 s b}{2}\left(C_{Y_0} + C_{Y_\beta}(\beta) + C_{Y_p}(\beta)\frac{b p}{2V} + C_{Y_r}\frac{b r}{2V}\right.\right. \\ & \left.\left. + C_{Y_{\delta a}}\delta a + C_{Y_{\delta r}}\delta r\right)\right]\sin\phi\end{aligned} \tag{81}$$

where:

$\Gamma_1 = \left(I_y - I_z\right)I_z - {I_{xz}}^2$, $\Gamma_2 = (I_x - I_y + I_z) - I_{xz}$

$\Gamma_5 = \frac{(I_z - I_x)}{I_y}$, $\Gamma_6 = \frac{(I_{xz})}{I_y}$, $\Gamma_7 = \frac{1}{I_y}$

and:
S = 0.3097m^2, c = 0.25, b =1.27 m, ρ = 1.19 at 100 ft. p = 4.25*10^{-25}, r =-4.173 *10^{-24}, ϕ =-0.0017, v = 17, θ= 0.0538, q =6.076*10^{-23}, β = -1.3714*10^{-22}, I_{xx}=0.0715, I_{yy}=0.0864, I_{zz}=0.1536,I_{xz} = 0.0140, C_{m_0}=-0.0278, $C_{m_\propto}$=-0.7230, C_{m_q}=-13.5664, $C_{m_{\delta e}}$=-0.8488, C_{Y_0} = 0.1, C_{Y_β}=-0.0545, $C_{Y_p}(\beta)$=-0.4496, C_{Y_r}=0.1086, $C_{Y_{\delta a}}$=-0.1646.

From the derivation of the linearization the obtained transfer function of pitch angle is given in equation 82

$$G_1(z) = \frac{\theta}{\delta e} = \frac{-0.0539\, z}{z^2 - 1.573z + 0.5729} \quad (82)$$

And transfer function of pitch rate is given in equation (83)

$$G_2(z) = \frac{q}{\delta e} = \frac{-2.655}{z - 0.5811} \quad (83)$$

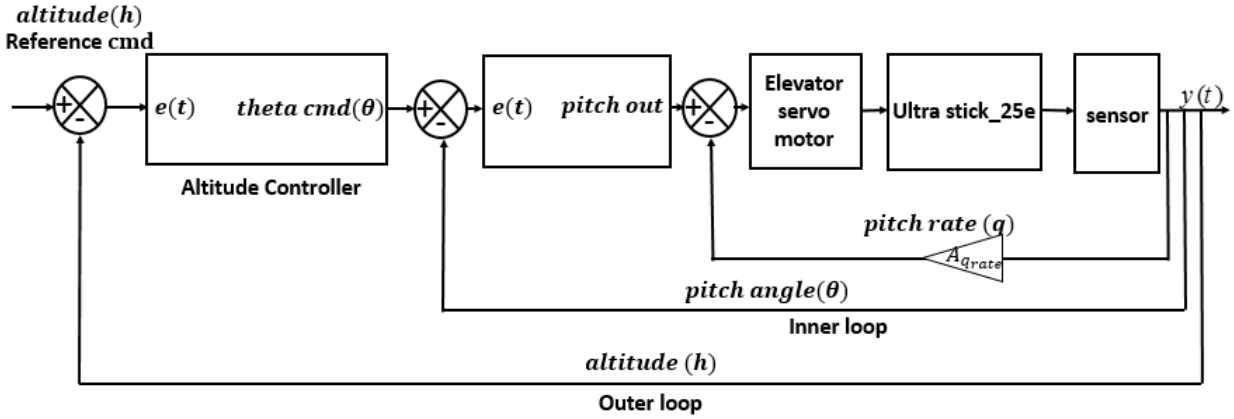

Figure 4. Longitudinal Autopilot

4. Flight control system design

Different tuning techniques for PI and PID controllers are used to enhance the performance and robustness of the autopilot regarding to the classical PI controller designed by university of Minnesota. The PI and PID are considered because of their simplicity to be implemented and their small execution time to produce the controller outputs as inputs for the actuators.

4.1. Genetically tuned (PI and PID) controller

Classical PI and PID controllers are implemented and genetically tuned to minimize an objective function. This objective function is the mean squared errors between the reference input and the system's output.

4.2. (PI and PID) Controllers optimizing by using LOC

A tuning method of digital PID and PI parameters is proposed using LOC as in [9, 10, 11]. To tune digital PI and PID controllers' parameters using LOC, the transfer function must be expressed as given in equation (84) and (85) respectively [12]. a, b In equation (84) and $a1, a2, b$ in equation (85) are the parameters of the linearized transfer function in first order and second order respectively.

$$G(z) = \frac{Y(z)}{U(z)} = \frac{b}{Z + a} \quad (84)$$

$$G(z) = \frac{Y(z)}{U(z)} = \frac{bZ}{Z^2 + a_1 Z + a_2} \tag{85}$$

For PID tuning using LOC, Kp, KI, and KD are given as in equation (86). For PI tuning using LOC, Kp, and KI are given as in equation (87).

PID/PI parameters tuned based on LOC are functions of model fixed value parameters and optimizable parameter h. The PI controller parameters of equation (87) are used to optimize the first order transfer function in (84) as pitch and roll rate transfer function as shown in Fig. 5 [13, 14]. The PID controller parameters of equation (86) are used to optimize the second order transfer function as pitch and roll angle transfer function as shown in Fig. 6 [15, 16].

$$K_p = \frac{-T_S(a_1 + a_2)}{b}, \quad K_I = \frac{T_S}{bh}, \quad K_D = \frac{a_2 T_S}{b} \tag{86}$$

$$K_p = \frac{-a T_S}{b}, \quad K_I = \frac{T_S}{bh} \tag{87}$$

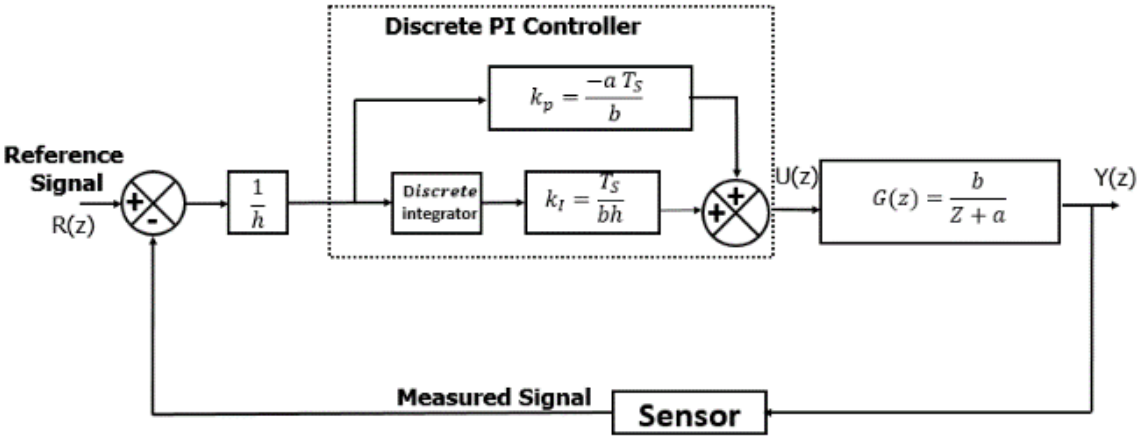

Figure 5. First order controller block diagram

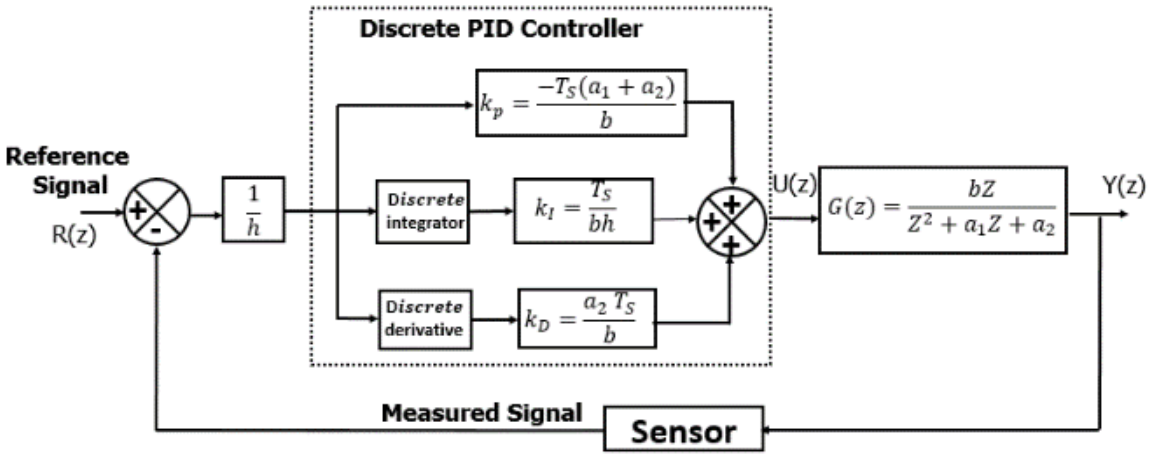

Figure 6. Second order controller block diagram

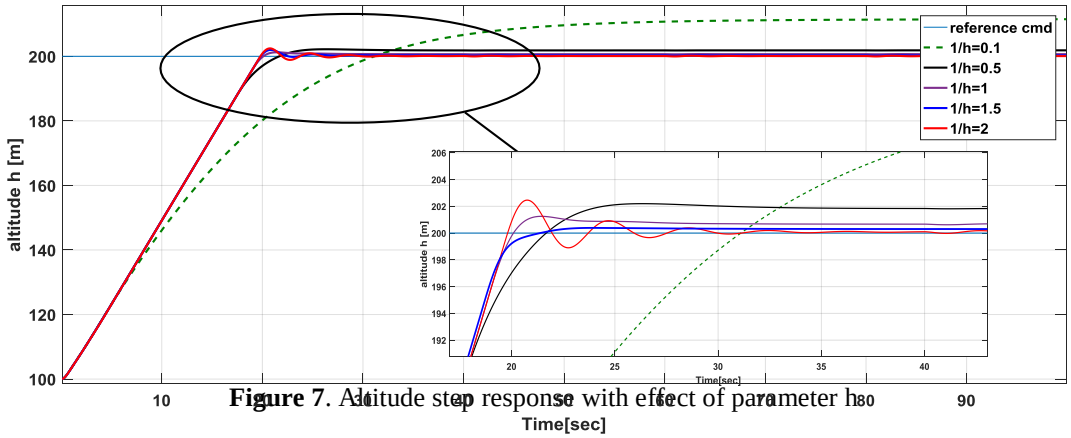

Figure 7. Altitude step response with effect of parameter h

Figure 7. Shows the step response of the altitude in nonlinear model at different values of parameter $1/h = [10,2,1,0.66,0.5]$.

The output response of pitch angle θ controlled in nonlinear system at different values of the tunable parameter $(1/h = 2.9,1,0.5,0.1)$ is shown in Fig. 8.

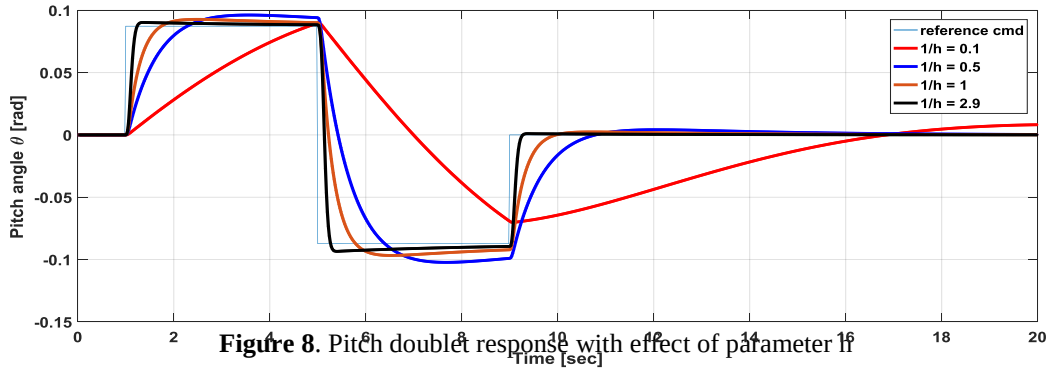

Figure 8. Pitch doublet response with effect of parameter h

The pitch rate q as an output response of the controlled nonlinear system at different values of the tunable parameter $(1/h = 10,5,2,1)$ is shown in Fig .9.

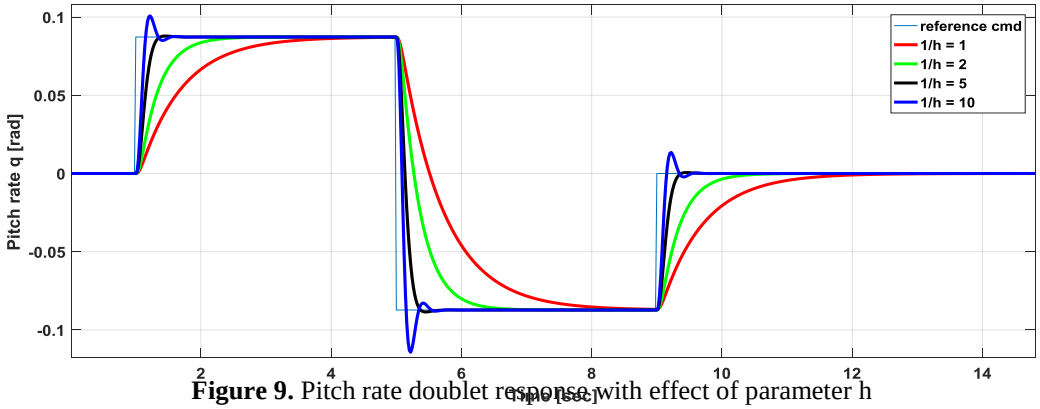

Figure 9. Pitch rate doublet response with effect of parameter h

The parameters of genetically tuned PID controller and the PID controller tuned using LOC for longitudinal channel are represented in Table 1. The Conventional PI designed by university of Minnesota is also represented in Table 1 to be compared with the two designed controllers.

Table 1. Longitudinal Controller parameters

controller	Conventional PID		Genetically tuned PID		PID tuned using LOC	
Pitch rate	$A_{q_{rate}}$	-0.1	$A_{q_{rate}}$	-0.1	$A_{q_{rate}}$	-0.171
Theta	KP	-0.751	KP	-0.901	KP	-0.84
	KI	-0.23	KI	-0.3015	KI	-0.35
			KD	0.001	KD	0.192

The parameters of genetically tuned PID controller and the PID controller tuned using LOC for lateral channel are represented in Table 2. The Conventional PI designed by university of Minnesota is also represented in Table 2 to be compared with the different designed controllers.

Table 2. Lateral Controller parameters

Controller	Conventional PID		Genetically tuned PID		PID tuned using LOC	
Roll rate	$A_{p_{rate}}$	-0.07	$A_{p_{rate}}$	-0.07	$A_{p_{rate}}$	-1.1
Phi	KP	-0.52	KP	-0.52	KP	-0.78
	Ki	-0.20	KI	-0.20	KI	-0.4
			KD	0.0018	KD	0.12

5. Simulation results and comparative study for linear model

The performance of the controlled system is analyzed for both longitudinal and lateral channels. The wind disturbance rejection and noise attenuation are considered as items for comparison beside the system performance.

5.1. Longitudinal channel

The genetically tuned PID controller and the PID tuned using LOC for longitudinal channel are compared with the conventional PI controller designed by university of Minnesota. The performance comparison of various control systems is set up by specifying particular test input signals and by comparing the various systems output responses to these input signals for linear model. The commonly used test input signal for pitch angle is multi-step input function, as shown in the Fig. 10.

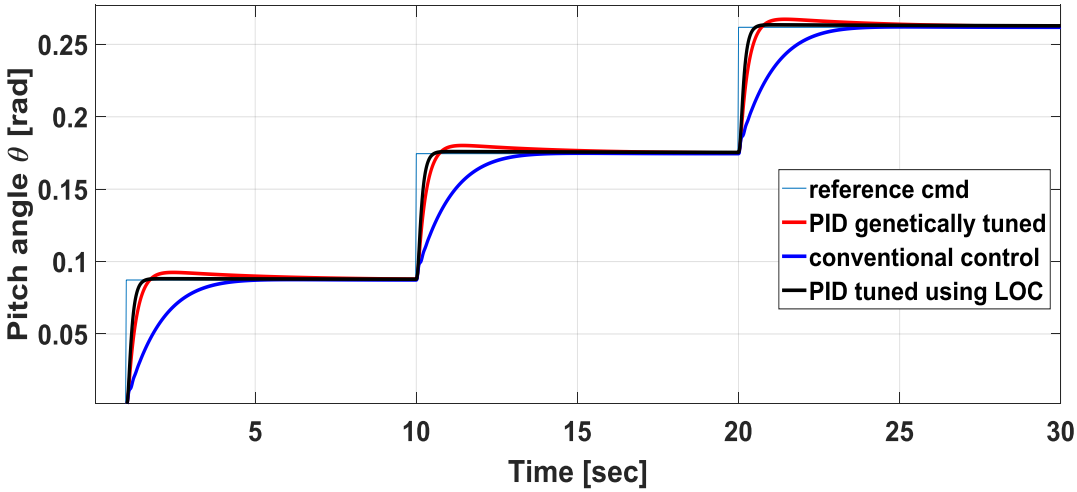

Figure 10. Multistep signal response for pitch tracker (linear model)

Fig. 10 illustrates the performance of the genetically tuned PID, and the PID tuned using LOC for linear model. The multi-step input signal is shown in figure. The reference Pitch angle changes from zero degree to +5, +10, +15 degree respectively. The output response of the system controlled by PID tuned using LOC is the best response followed by system controlled by genetically tuned PID. The worst response is the conventional PI controller designed by university of Minnesota. The rise time, settling time, and steady state error of tuning of PID using local optimal control are better than the corresponding ones of the two other controllers compared.

The rejection of the wind disturbance is examined for the step response after reaching steady state. Fig. 11 shows that the wind disturbance is applied after 10 seconds. The response of the system at this time is at steady state for each controller. From this figure, it is clear that the wind disturbance rejection of the system controlled by PID tuned using LOC is better than the genetically tuned PID. The worst wind disturbance rejection is for the conventional PI designed by University of Minnesota. The PID tuned using LOC is smoother and faster in disturbance rejection.

The effect of sensors noise with $\frac{\mathrm{N}}{\mathrm{S}} = 10\%$ can be considered for the pitch tracker and altitude hold controller as seen from Fig. 12 and Fig. 13 respectively. Fig. 12 shows that the best noise mitigation for pitch tracker is obtained by PID tuned using LOC followed by the genetically tuned PID. Fig. 13 shows that the best noise mitigation for altitude hold is obtained also by PID tuned using LOC followed by the genetically tuned PID. The worst case is for the conventional PI designed by University of Minnesota.

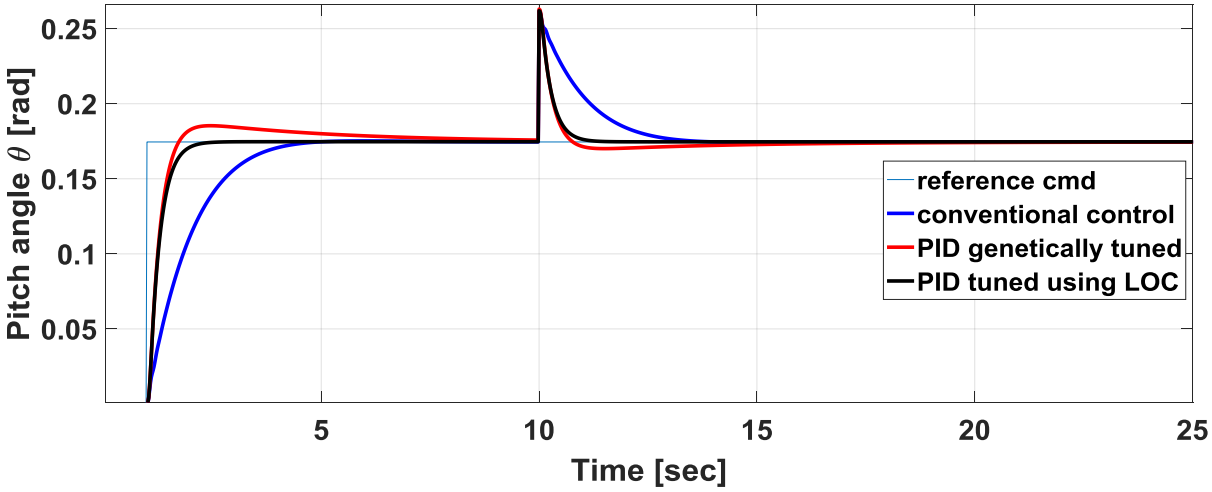

Figure 11. The ability of pitch tracker to deal with wind disturbance

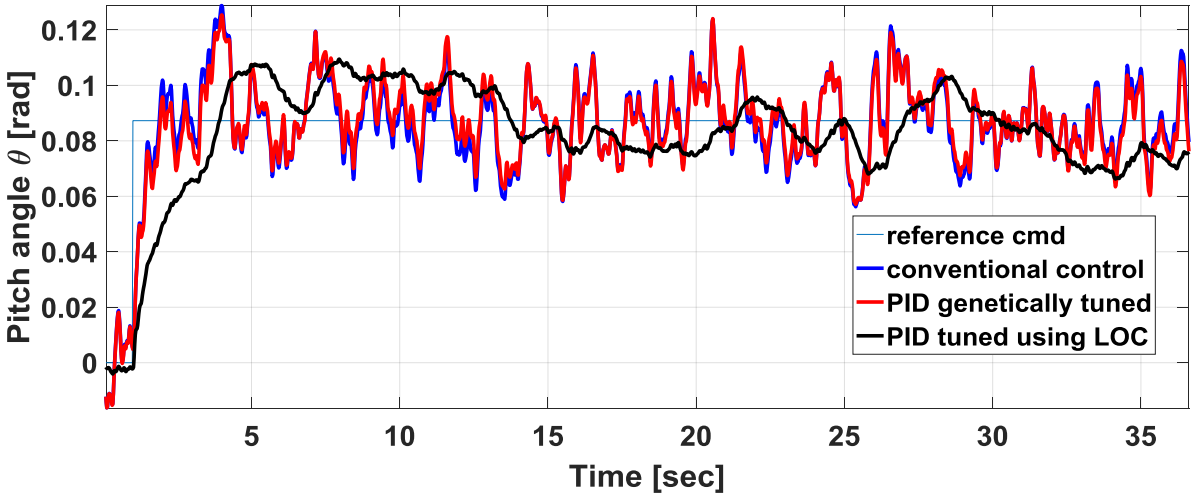

Figure 12. Noise effect in the step signal for pitch angle 5[deg]

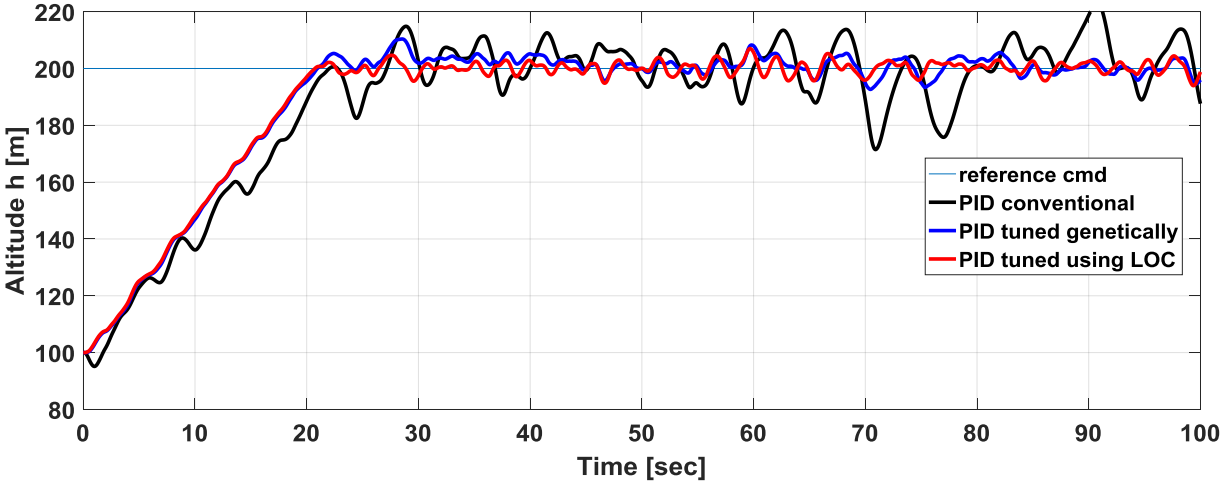

Figure 13. Noise effect in the step signal for altitude 100m

5.2. Lateral channel

The genetically tuned PID controller and the PID controller tuned using LOC for lateral channel are compared with the conventional PI controller designed by university of Minnesota. The performance comparison of various control systems is set up by specifying particular test input signals and by comparing the various systems output responses to these input signals for linear model. The commonly used test input signal is doublet response function for roll angle, as shown in the Fig. 14. It illustrates the performance of the genetically tuned PID, and the PID controller tuned using LOC for linear model. The reference roll angle changes from zero degree to +5 degree, then to -5 degree, and finally to zero degree. The output responses of the system controlled by PID controller tuned using LOC is better than genetically tuned PID controller. The worst response is the conventional PI controller designed by university of Minnesota. The rise time, settling time, and steady state error of PID controller tuned using LOC are better than the corresponding ones of the two other controllers compared.

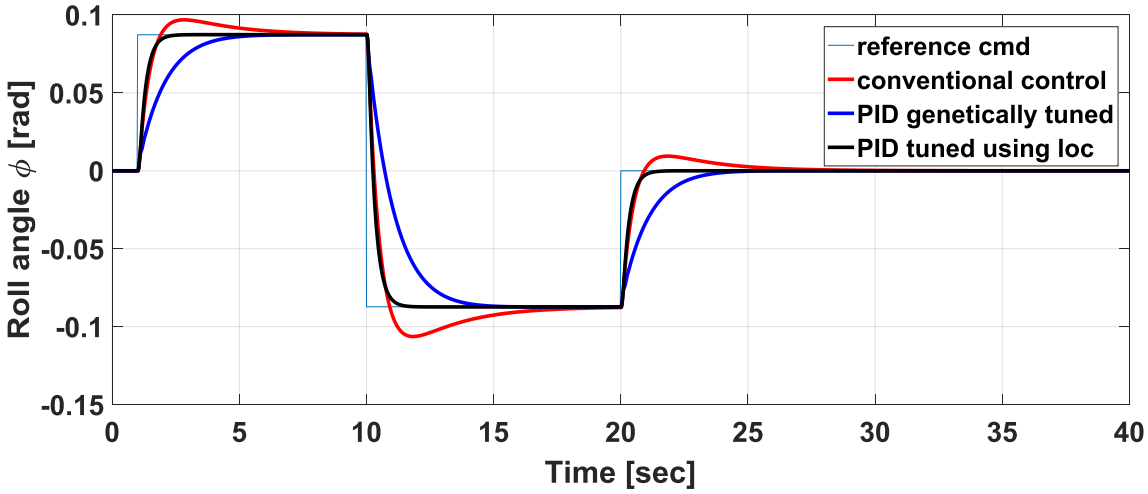

Figure 14. Doublet response for roll angle (linear model)

The rejection of the wind disturbance is examined for the step response after reaching steady state. Fig. 15 shows that, the wind disturbance is applied after 10 seconds. The response of the system at this time is at steady state for each controller. From this figure, it is clear that the wind disturbance rejection of the system controlled by PID tuned using LOC is better than the genetically tuned PID. The worst wind disturbance rejection is for the conventional PI designed by University of Minnesota. The PID tuned using LOC is smoother and faster in disturbance rejection.

The noise effect with $\frac{N}{S} = 10\%$ can be considered for the roll tracker and heading angle controller as seen from Fig. 16. And Fig. 17 It shows that the better noise mitigation for roll tracker and heading angle respectively is obtained by the PID tuned using LOC followed by the genetically tuned PID.

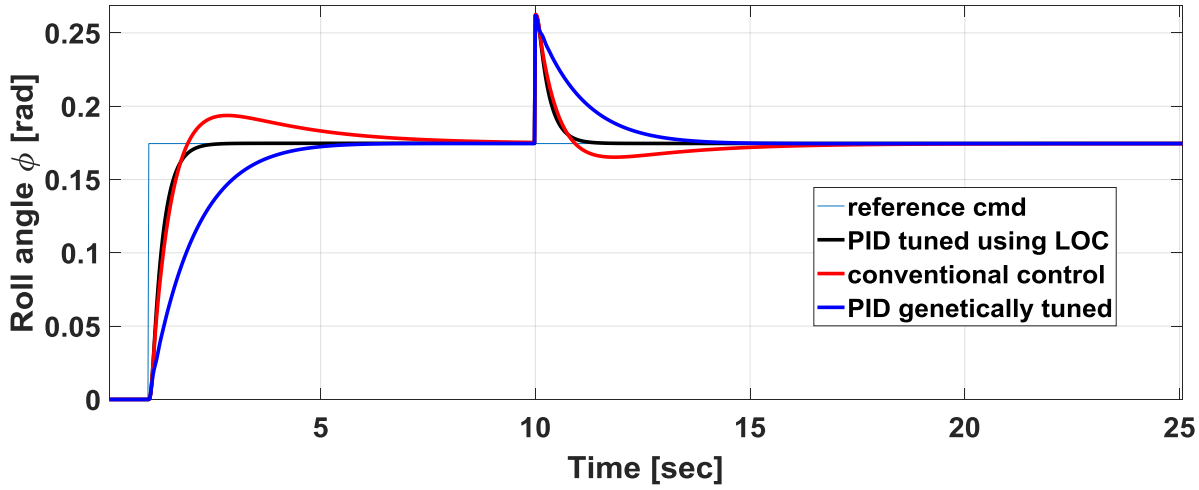

Figure 15. The ability of roll tracker to deal with wind disturbance

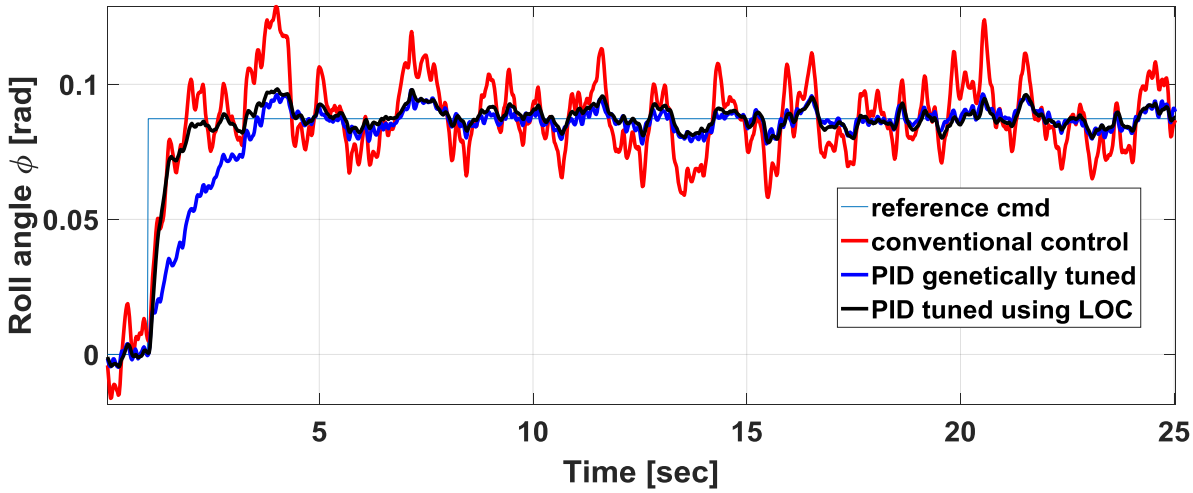

Figure 16. Noise effect in the step signal response for roll angle 5[deg]

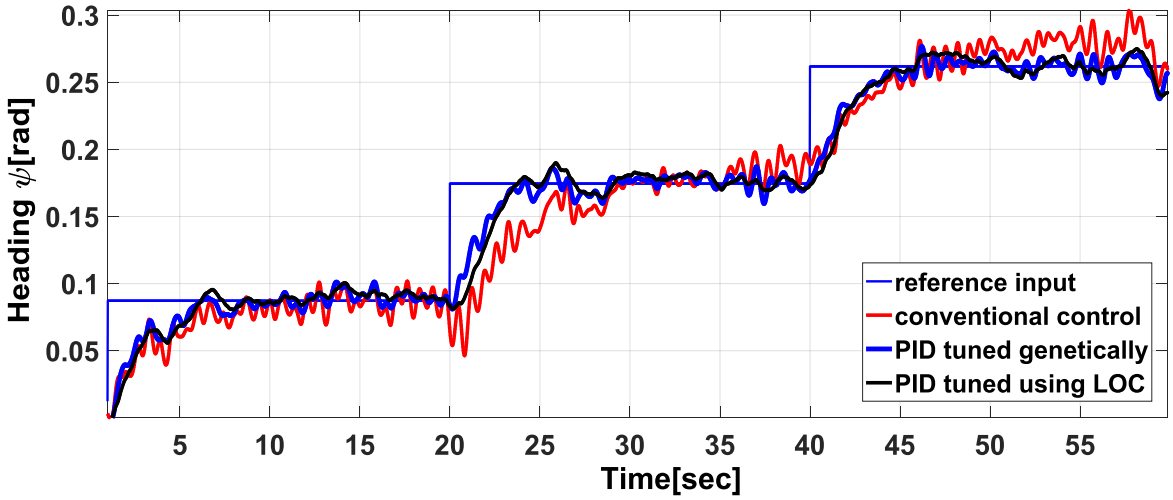

Figure 17. Noise effect in the Multistep response for heading angle (+5, +10, +5) [deg]

6. Simulation results and comparative study for nonlinear model

After obtaining acceptable control response for linear model, the designed controllers are applied for nonlinear model. A comparative study is held between the designed controllers. This is can be considered as robustness to model uncertainties. This is because the controllers are designed for the linear model and tested for the nonlinear model.

6.1. Longitudinal channel

Fig. 18 shows the output response of each controlled system for altitude step input of 100 m. This Figure illustrates that, the PID optimized by using LOC is better than PID controller genetically tuned, and conventional PI controller designed by University of Minnesota. The PID optimized by using LOC has the smallest over-shoot, fastest settling time, and no steady state error

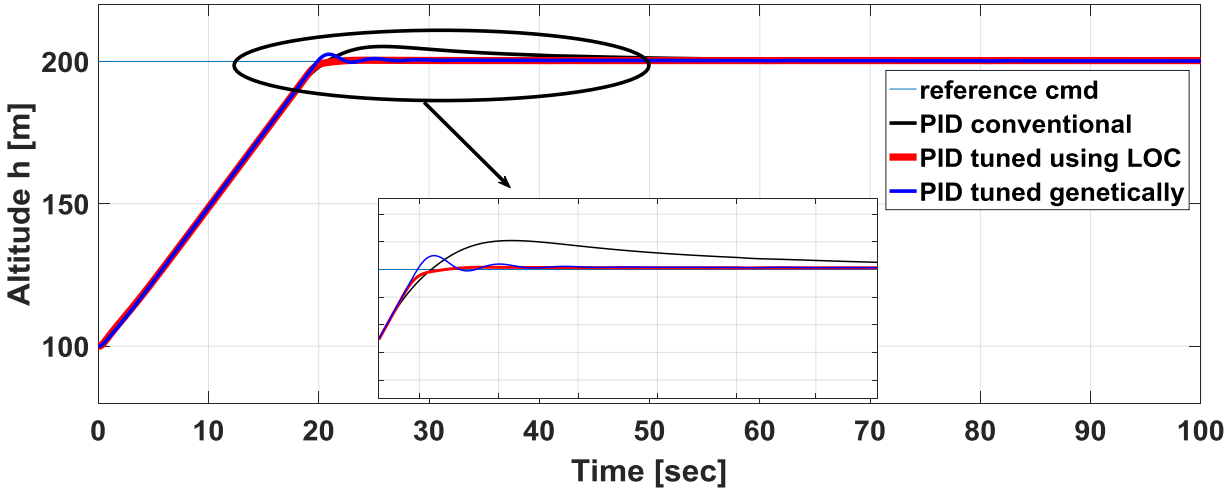

Figure 18. Level climbs scenario100m altitude from pitch (nonlinear model)

6.2. Lateral channel

Fig. 19 shows the output response of each controlled system for heading angle multistep input. This Figure illustrates that, the PID optimized by using LOC is better than PID controller genetically tuned, and conventional PI controller designed by University of Minnesota. The PID tuned using LOC has the smallest overshoot, fastest settling time, and no steady state error

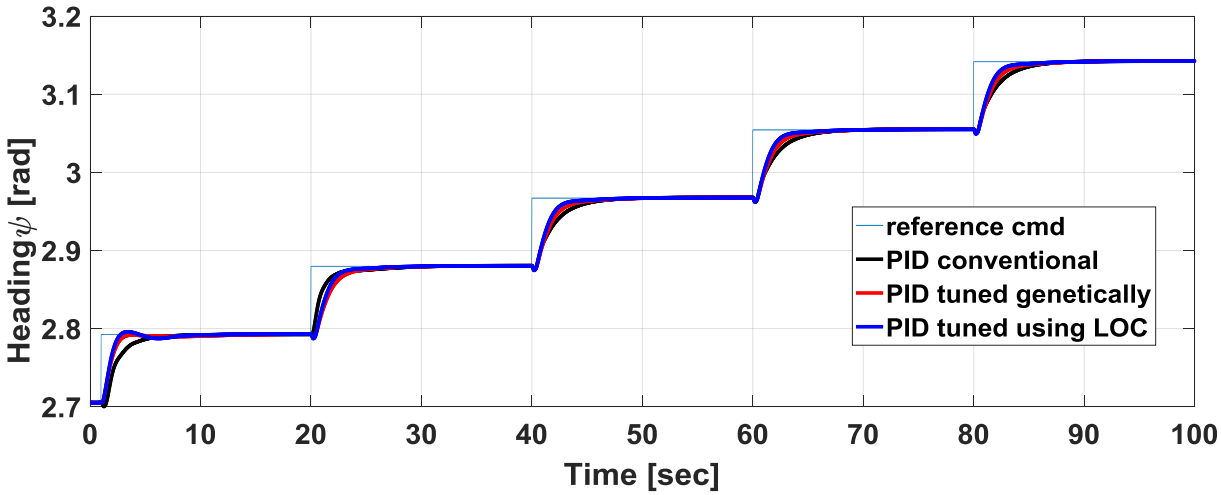

Figure 19. Multistep signal response for heading tracker (nonlinear model)

7. Conclusion

Mathematical nonlinear model for fixed wing Ultrastick-25e UAV is derived from the first principles. The obtained nonlinear model is linearized for simplicity and to be used in control purposes. Genetically tuned PID controller and PID optimized based on LOC are designed for multivariable controller of Ultrastick-25e UAV in both lateral and longitudinal channels. Traditional PI controller designed by university of Minnesota is compared with the underlying controllers. The triple proposed controllers are utilized for the linear model of the Ultrastick-25e. The PID tuned based on LOC achieves a superior output response compared with both channels even in the presence of disturbance and noise. After the different controllers are designed for linearized model, the proposed controllers are applied to the nonlinear model to test the system robustness of every controller considering the model uncertainties. The PID tuned based on LOC achieves the superior robust performance and stability in the presence of the model uncertainty.

References

[1] A. N. Oda, G. A. El-Sheikh, Y. Z. El-Halwagy, M. Ashry, "Robust CLOS Guidance and Control: Part-1: System Modeling and Uncertainty Evaluation" *14th International Conference on aerospace sciences and aviation technology, Military Technical College, 2011, Cairo, Egypt.*

[2] A. N. Oda, G. A. El-Sheikh, Y. Z. El-Halwagy, M. Ashry, "Robust CLOS Guidance and Control: Part-2: Scalar H-infinity Autopilot Synthesis" 14th *International Conference on aerospace sciences and aviation technology, Military Technical College, 2011, Cairo, Egypt.*

[3] A. N. Oda, G. A. El-Sheikh, M. Ashry, Y. Z. El-Halwagy, M. A. Abd-Altief, "Robust CLOS Guidance and Control: Part-3:HIL Systems Simulation" *14th International Conference on aerospace sciences and aviation technology, Military Technical College, 2011, Cairo, Egypt.*

[4] A. Sarhan, M. Ashry, "Self-Tuned PID Controller for the Aerosonde UAV Autopilot" International Journal of Engineering Research & Technology (IJERT), Vol 2, Issue 12, PP: 3329-3340, Dec. 2013

[5] Y. Z. Elhalwagy, M. Tarbochi, "Integration of fuzzy guidance-control system for a command interceptor against hypersonic target" *IECON proceeding (industrial electronics conference), 2001, Denver, Colorado, USA.*

[6] M. Mahfouz, A. T. Hafez, M. Ashry, G. Elnashar, "Formation configuration for cooperative multiple UAV via backstepping PID controller" *2018 AIAA SPACE and Astronautics Forum and Exposition, 2018, Florida, USA.*

[7] Eslam n.mobarez, A. N. Ouda "Mathematical Representation, Modeling and Linearization for Fixed Wing UAV'' *international journal of computer application Volume 147 – No.2, August 2016.*

[8] A. Elsayed Ahmed, "Modeling of a Small Unmanned Aerial Vehicle," World Academy of Science, Engineering and Technology International Journal of Mechanical, Aerospace, Industrial, Mechatronic and Manufacturing Engineering Vol: 9, No: 3, 2015

[9] Ahmed Elsayed, A. N. Ouda, Ashraf Hafez "Design of a longitudinal Motion Controller for a Small Unmanned Aerial Vehicle (SUAV)," *I. J. Intelligent Systems and Applications, Vol 10, PP: 37-47, 2015.*

[10] Amr Sarhan and Shiyin Qin "Adaptive PID Control of UAV Altitude Dynamics Based On Parameter Optimization with Fuzzy Inference," *International Journal of Modeling and Optimization, Vol. 6, No. 4, August 2016.*

[11] M. Ashry, U. Abou-Zayed, and T. Breikin, "Control of multivariable systems using modified local optimal controller", *The 17th IFAC world congress, Seoul, Korea, 2008.*

[12] U. Abou-Zayed, M. Ashry, T. Breikin, "Implementation of local optimal controller based on model identification of multi-mass electromechanical servo system" *IASTED International Conference on Modelling, Identification, and Control, Innsbruck, Austria, 2008.*

[13] M. Ashry, U. Abou-Zayed, and T. Breikin, "Comparative robustness study of multivariable controllers for a gas turbine engine", *IASTED International Conference on Modelling, Identification, and Control, Innsbruck, Austria, 2008.*

[14] Abou-Zayed, U., Ashry, M., Breikin, T. "Experimental open-loop and closed-loop identification of a multi-mass electromechanical servo system" *ICINCO 2008 - 5th International Conference on Informatics in Control, Automation and Robotics, Madeira, Portugal, 2008.*

[15] Ashry, M.M., Kamalova, Z.Z., Breikin, T.V. "Tuning of digital PID controller parameters using local optimal control" *16th Mediterranean Conference on Control and Automation, MED'08, Ajaccio, France, 2008.*